

Cobalt(III)/Cobalt(II) Electrochemical Potential Controlled by Steric Constraints in Self-Assembled Dinuclear Triple-Helical Complexes

Claude Piguet,[†] Gérald Bernardinelli,[‡] Bernard Bocquet,[†] Olivier Schaad,[§] and Alan F. Williams^{*†}

Department of Inorganic, Analytical and Applied Chemistry, Laboratory of X-ray Crystallography, and Department of Biochemistry, University of Geneva, CH-1211 Geneva 4, Switzerland

Received September 17, 1993[⊙]

The ligands bis[5-(1-methyl-2-(X'-methyl-2'-pyridyl)benzimidazolyl)]methane (X' = 6', 6-bisbmbmp, **1**; X' = 5', 5-bisbmbmp, **2**) react with cobalt(II) perchlorate in acetonitrile to give self-assembled dinuclear triple-helical complexes. The crystal structures of [Co₂(6-bisbmbmp)₃](ClO₄)₄(CH₃CN)_{2.5} (**6**, Co₂C₉₂H_{85.5}N_{20.5}Cl₄O₁₆, *a* = 14.403(2) Å, *b* = 16.558(3) Å, *c* = 21.328(3) Å, α = 78.15(1)°, β = 81.19(1)°, γ = 89.02(1)°, triclinic, P $\bar{1}$, Z = 2) and [Co₂(5-bisbmbmp)₃](ClO₄)₄(CH₃CN)₆ (**7**, Co₂C₉₉H₉₆N₂₄Cl₄O₁₆, *a* = 13.648(5) Å, *b* = 16.917(4) Å, *c* = 22.801(8) Å, α = 92.45(1)°, β = 103.80(1)°, γ = 96.32(1)°, triclinic, P $\bar{1}$, Z = 2) show dinuclear triple-helical cations [Co₂(6-bisbmbmp)₃]⁴⁺ and [Co₂(5-bisbmbmp)₃]⁴⁺ where the three bidentate ligands are wrapped around a pseudo-C₃ axis defined by the cobalt atoms. The coordination spheres around the high-spin cobalt(II) ions may best be described as octahedra flattened along the C₃ axis. Comparison of the structures shows that steric repulsions between the methyl groups in the 6-positions of the pyridine rings in **6** result in a distortion of the coordination spheres around Co(II) and increase in the Co–N(py) bond distances. ¹H-NMR and electronic spectra and spectrophotometric titrations in solution indicate that the pseudo-D₃ triple-helical structures of [Co₂(6-bisbmbmp)₃]⁴⁺ and [Co₂(5-bisbmbmp)₃]⁴⁺ are maintained in acetonitrile and result from cooperative self-assembly processes. The greater deformation of the coordination spheres around Co(II) in [Co₂(6-bisbmbmp)₃]⁴⁺ is responsible for a decrease of the stability of the triple-helical structure in solution and the failure to observe the oxidation of Co(II) in [Co₂(6-bisbmbmp)₃]⁴⁺.

Introduction

The use of self-assembly processes¹ based on complexation reactions^{2–4} for the selective formation of three-dimensional supramolecular architectures has become a theme of considerable interest in the design of organized molecular structures^{2–5} and supramolecular devices.^{4–6} Particular attention has been focused on the formation of helical complexes (helicates) obtained by the self-assembly of oligo-multidentate ligands with various metal ions.^{7–9} Double-helical structures may be generated by the complexation of two ligands twisted around the metal ions lying

on the helical axis, and many such dinuclear systems have been synthesized from oligo-multidentate ligands based on 2,2'-bipyridine,^{9–12} 1,10 phenanthroline,^{11,13,14} 2,2':6',2'' terpyridine,¹⁵ or analogous terdentate units¹⁶ with Cu(I), Ag(I), Ru(II), and Fe(II). Lehn and his collaborators have synthesized double helicates which contain up to five Cu(I) ions and show positive cooperativity in the self-assembly process,¹⁷ while Constable⁷ has used polypyridyl ligands to develop a rich and varied chemistry of double-helical complexes with many metal ions. Among the conditions required for the self-assembly of helical complexes, two main points appear to be essential if these processes are to give predictable products.^{18,19} First, the ligand should possess well-defined metal binding sites (mono-, bis-, or terdentate) separated by a spacer which arranges them in such a way as to favor the formation of polynuclear complexes. Second, the binding possibilities of the ligand should match the stereochemical preferences of the metal ions which then control the final structure adopted by the complex. Following these criteria, we have

[†] Department of Inorganic, Analytical and Applied Chemistry, University of Geneva.

[‡] Laboratory of X-ray Crystallography, University of Geneva.

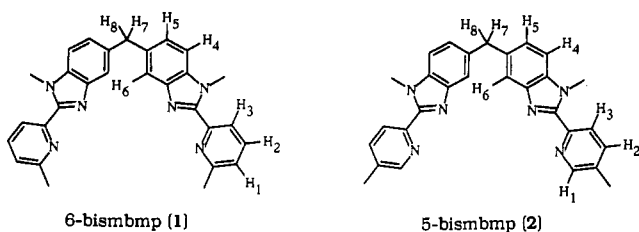
[§] Department of Biochemistry, University of Geneva.

[⊙] Abstract published in *Advance ACS Abstracts*, July 15, 1994.

- (1) Lindsey, J. S. *New J. Chem.* **1991**, *15*, 153–180.
- (2) (a) Lehn, J.-M. *Angew. Chem., Int. Ed. Engl.* **1990**, *29*, 1304–1319. (b) Baxter, P.; Lehn, J.-M.; DeCian, A.; Fischer, J. *Angew. Chem., Int. Ed. Engl.* **1993**, *32*, 69–72.
- (3) Seel, C.; Vögtle, F. *Angew. Chem., Int. Ed. Engl.* **1992**, *31*, 528–549.
- (4) Balzani, V. *Tetrahedron* **1992**, *48*, 10443–10514.
- (5) Anelli, P. L.; Ashton, P. R.; Ballardini, R.; Balzani, V.; Delgado, M.; Gandolfi, M. T.; Goodnow, T. T.; Kaifer, A. E.; Philip, D.; Pietraszkiewicz, M.; Prodi, L.; Reddington, M. V.; Slawin, A. M. Z.; Spencer, N.; Stoddart, J. F.; Vicent, C.; Williams, D. J. *J. Am. Chem. Soc.* **1992**, *114*, 193–218.
- (6) Collin, J.-P.; Guillerez, S.; Sauvage, J.-P.; Barigoletti, F.; De Cola, L.; Flamigni, L.; Balzani, V. *Inorg. Chem.* **1992**, *31*, 4112–4117.
- (7) Constable, E. C. *Tetrahedron* **1992**, *48*, 10013–10059.
- (8) Constable, E. C. *Nature* **1990**, *346*, 314–315.
- (9) Lehn, J.-M.; Sauvage, J.-P.; Simon, J.; Ziessel, R.; Piccini-Leopardi, C.; Germain, G.; Declercq, J.-P.; Van Meerssche, M. *Nouv. J. Chim.* **1983**, *7*, 413–420. Gisselbrecht, J.-P.; Gross, M.; Lehn, J.-M.; Sauvage, J.-P.; Simon, J.; Ziessel, R.; Piccini-Leopardi, C.; Arrieta, J. M.; Germain, G.; Van Meerssche, M. *Nouv. J. Chim.* **1984**, *8*, 661–667. Lehn, J.-M.; Rigault, A.; Siegel, J.; Harrowfield, J.; Chevrier, B.; Moras, D. *Proc. Natl. Acad. Sci. U.S.A.* **1987**, *84*, 2565–2569. Lehn, J.-M.; Rigault, A. *Angew. Chem., Int. Ed. Engl.* **1988**, *27*, 1095–1097. Koert, U.; Harding, M. M.; Lehn, J.-M. *Nature* **1990**, *346*, 339–342. Harding, M. M.; Koert, U.; Lehn, J.-M.; Piguet, C.; Rigault, A.; Siegel, J. *Helv. Chim. Acta* **1991**, *74*, 594–610. Garrett, T. M.; Koert, U.; Lehn, J.-M.; Rigault, A.; Meyer, D.; Fischer, D. *J. Chem. Soc., Chem. Commun.* **1990**, 557–558.

- (10) Zarges, W.; Hall, J.; Lehn, J.-M. *Helv. Chim. Acta* **1991**, *74*, 1843–1852.
- (11) Youinou, M.-T.; Ziessel, R.; Lehn, J.-M. *Inorg. Chem.* **1991**, *30*, 2144–2148.
- (12) Serr, B. R.; Andersen, K. A.; Elliott, C. M.; Anderson, P. O. *Inorg. Chem.* **1988**, *27*, 4499–4504.
- (13) (a) Sauvage, J.-P. *Acc. Chem. Res.* **1990**, *23*, 319–327. (b) Dietrich-Bücheker, C. O.; Guilhem, J.; Pascard, C.; Sauvage, J.-P. *Angew. Chem., Int. Ed. Engl.* **1990**, *29*, 1154–1156. (c) Dietrich-Bücheker, C. O.; Sauvage, J.-P.; Kintzinger, J.-P.; Maltête, P.; Pascard, C.; Guilhem, J. *New J. Chem.* **1992**, *16*, 931–942.
- (14) Yao, Y.; Perkovic, M. W.; Rillema, D. P.; Woods, C. *Inorg. Chem.* **1992**, *31*, 3956–3962.
- (15) Crane, J. D.; Sauvage, J.-P. *New J. Chem.* **1992**, *16*, 649–650.
- (16) Piguet, C.; Bernardinelli, G.; Williams, A. F. *Inorg. Chem.* **1989**, *28*, 2920–2925. Rüttimann, S.; Piguet, C.; Bernardinelli, G.; Bocquet, B.; Williams, A. F. *J. Am. Chem. Soc.* **1992**, *114*, 4230–4237.
- (17) Pfeil, A.; Lehn, J.-M. *J. Chem. Soc., Chem. Commun.* **1992**, 838–840. Garrett, T. M.; Koert, U.; Lehn, J.-M. *J. Phys. Org. Chem.* **1992**, *5*, 529–532.
- (18) Piguet, C.; Bernardinelli, G.; Bocquet, B.; Quattropiani, A.; Williams, A. F. *J. Am. Chem. Soc.* **1992**, *114*, 7440–7451.
- (19) Krämer, R.; Lehn, J.-M.; De Cian, A.; Fischer, J. *Angew. Chem., Int. Ed. Engl.* **1993**, *32*, 703–706.

previously reported the selective formation of a double-helical complex $[\text{Co}_2(6\text{-bismbmp})_2]^{2+}$ or a triple-helical complex $[\text{Co}_2(6\text{-bismbmp})_3]^{4+}$ with the same bis-bidentate ligand.^{18,20} Surprisingly, we were unable to oxidize the octahedral Co(II) complex $[\text{Co}_2(6\text{-bismbmp})_3]^{4+}$ on a platinum disk electrode even though Co(III) displays a pronounced stereochemical preference for octahedral coordination.²¹ Since the preparation of a kinetically inert²² low-spin d^6 Co(III) triple helical complex should allow the separation of the two helical enantiomers, this was a disappointing result. We decided to investigate the reasons for the failure of the Co(II) complex to oxidize and present here the preparation of the new bis-bidentate ligand bis[5-(1-methyl-2-(5'-methyl-2'-pyridyl)benzimidazolyl)]methane (5-bismbmp, **2**) which differs



from the analogous 6-bismbmp (**1**) only by the positions of the methyl groups bound to the pyridine rings, and we report the chemistry of these ligands with Co(II). A partial report of the crystal structure of the triple-helical complex $[\text{Co}_2(6\text{-bismbmp})_3](\text{ClO}_4)_4 \cdot 2.5\text{CH}_3\text{CN}$ (**6**) has already been published as a preliminary communication,²⁰ and we give here the complete description of the crystal structure of this complex and that of the new analogous complex $[\text{Co}_2(5\text{-bismbmp})_3](\text{ClO}_4)_4 \cdot 6\text{CH}_3\text{CN}$ (**7**). Comparison of the two structures shows that the position of the methyl groups on the pyridine moieties can strongly influence the chemistry of the complexes.

Experimental Section

Solvents and starting materials were purchased from Fluka AG (Buchs, Switzerland) and used without further purification, unless otherwise stated. Aluminum oxide (Merck activity II–III, 0.063–0.200 mm) was used for preparative column chromatography.

Preparation of the Ligands. (3,3'-Diamino-4,4'-bis(*N*-methylamino)-diphenyl)methane (**5**) and the ligand bis[5-(1-methyl-2-(6'-methyl-2'-pyridyl)benzimidazolyl)]methane (6-bismbmp, **1**) were prepared according to literature procedures.¹⁸

Preparation of 2-Carboxy-5-methylpyridine (3). 2,5-Lutidine (10 g, 93.3 mmol) and selenium dioxide (15.54 g, 140 mmol) were refluxed in pyridine (60 mL) under a nitrogen atmosphere for 36 h. After cooling, the solution was filtered and the solid residue was washed with pyridine (60 mL) and then with water (60 mL). The resulting solution was distilled in steam (500 mL of water), and the remaining aqueous phase was filtered on Celite, evaporated, and dried under vacuum. The crude residue was suspended in dry ethanol (400 mL) containing concentrated sulfuric acid (6 mL), and then the mixture was refluxed for 15 h under an inert atmosphere. The mixture was hydrolyzed with water (100 mL) and neutralized to pH = 7.0 with aqueous 5 M NaOH, and ethanol was evaporated. The aqueous phase was extracted with dichloromethane (2 × 200 mL); the combined organic phases were dried on cellulose, and the solvent was evaporated. The crude liquid was distilled (67 °C/0.5 Torr) to give 7.47 g (45.22 mmol; yield = 48%) of colorless 2-carboxy-5-methylpyridine (**3**). Bp: 131 °C/10 mmHg. ¹H-NMR in CDCl₃: 1.42 (3H, t, $J^3 = 7$ Hz), 2.39 (3H, s), 4.44 (2H, quart, $J^3 = 7$ Hz), 7.60 (1H, d, d, quart., $J^3 = 8$ Hz, $J^4(\text{H-H}) = 2.2$ Hz, $J^4(\text{H-CH}_3) = 0.7$ Hz), 8.01 (1H, d, $J^3 = 8$ Hz), 8.55 (1H, d, quart., $J^4(\text{H-H}) = 2.2$ Hz, $J^4(\text{H-CH}_3) = 0.8$ Hz). EI-MS: *m/e* 165 (M⁺), 92 ([M - CO₂Et]⁺).

Preparation of 2-Carboxy-5-methylpyridine (4). 2-Carboxy-5-methylpyridine (**3**) (8 g, 48 mmol) and potassium hydroxide (9.51 g, 144 mmol) were dissolved in ethanol/water (1:1; 300 mL). The mixture was refluxed for 1 h, and the ethanol was then evaporated. The resulting basic aqueous phase was extracted with dichloromethane (200 mL), neutralized to pH = 3.5 with concentrated hydrochloric acid, and evaporated to dryness. The crude residue was extracted with hot ethyl acetate (700 mL) for 3 h, the hot organic phase was filtered, and ethyl acetate was slowly evaporated to allow crystallization. After cooling of the solution to -20 °C, 6.1 g (44.5 mmol; yield = 92%) of 2-carboxy-5-methylpyridine was obtained as white crystals. Mp: 163–165 °C (lit.²³ mp 167–168 °C). ¹H-NMR in CD₃OD: 2.44 (3H, s), 7.86 (1H, d, d., $J^3 = 8$ Hz, $J^4 = 2$ Hz), 8.06 (1H, d, $J^3 = 8$ Hz), 8.45 (1H, s, broad). EI-MS: *m/e* 137 (M⁺), 93 ([M - CO₂]⁺).

Preparation of Bis[5-(1-methyl-2-(5'-methyl-2'-pyridyl)benzimidazolyl)]methane (5-bismbmp, **2).** (3,3'-Diamino-4,4'-bis(*N*-methylamino)-diphenyl)methane (**5**)¹⁸ (1.96 g, 7.65 mmol) and 2-carboxy-5-methylpyridine (**4**) (3.25 g, 22.9 mmol) were dissolved in methanol (20 mL), the solution was transferred in a glass tube, and the solvent was evaporated. The solid residue was dried under vacuum, and the glass tube was sealed and then heated at 170 °C for 36 h. After cooling of the solution to room temperature, the dark red solid was extracted with dichloromethane (2 × 100 mL). The combined organic phases were dried on cellulose and evaporated. The crude residue was purified by column chromatography (Al₂O₃; CH₂Cl₂/MeOH, 98.5:1.5) and then crystallized from acetonitrile to give 2.93 g (6.33 mmol, yield = 84%) of bis[5-(1-methyl-2-(5'-methyl-2'-pyridyl)benzimidazolyl)]methane (5-bismbmp, **2**) as white needles. Mp: 192 °C dec. ¹H-NMR in CDCl₃: 2.39 (6H, s, broad), 4.22 (6H, s), 4.27 (2H, s), 7.20 (2H, d, d, $J^3 = 8.4$ Hz, $J^4 = 1.5$ Hz), 7.30 (2H, d, d, $J^3 = 8.4$ Hz, $J^5 = 0.7$ Hz), 7.64 (2H, d, d, quart., $J^3 = 8.1$ Hz, $J^4(\text{H-H}) = 2.2$ Hz, $J^4(\text{H-CH}_3) = 0.6$ Hz), 7.68 (2H, d, d, $J^4 = 1.5$ Hz, $J^5 = 0.6$ Hz), 8.25 (2H, d, d, $J^3 = 8.1$ Hz, $J^5 = 0.6$ Hz), 8.50 (2H, m). ¹³C-NMR in CDCl₃: 18.31, 32.53 (primary C); 42.18 (secondary C); 109.56, 119.66, 124.05, 124.42, 137.16, 148.79 (tertiary C); 133.28, 135.73, 136.21, 142.72, 148.00, 150.42 (quaternary C). EI-MS: *m/e* 458 (M⁺).

Preparation of Cobalt(II) Complexes. $[\text{Co}_2(6\text{-bismbmp})_3](\text{ClO}_4)_4 \cdot 3\text{H}_2\text{O}$ was prepared according to a previously published procedure.¹⁸

Preparation of $[\text{Co}_2(5\text{-bismbmp})_3](\text{ClO}_4)_4 \cdot 4\text{H}_2\text{O}$. A solution of 5-bismbmp (**2**) (0.2 g, 0.44 mmol) in dichloromethane (10 mL) was added to a solution of Co(ClO₄)₂·6H₂O (0.106 g, 0.29 mmol) in acetonitrile (10 mL). The yellow mixture was evaporated to dryness, the solid was dissolved in acetonitrile (2 mL), and methanol was slowly diffused into the solution for 3 days. Orange prisms of quality suitable for X-ray diffraction measurements were separated and dried to give 0.22 g (0.112 mmol, yield = 77%) of $[\text{Co}_2(5\text{-bismbmp})_3](\text{ClO}_4)_4 \cdot 4\text{H}_2\text{O}$. ¹H-NMR in CD₃CN: -40.2 (6H, s), -4.2 (6H, s), -0.7 (18H, s), 1.7 (6H, s), 12.6 (6H, s), 14.7 (18H, s), 33.4 (6H, s), 59.8 (6H, s), 80.6 (6H, s). ES-MS: *m/e* 373.2 ([Co₂(5-bismbmp)₃]⁴⁺). Anal. Calcd for Co₂C₈₇H₇₈N₁₈Cl₄O₁₆·4H₂O: Co, 6.00; C, 53.22; N, 12.84; H, 4.41. Found: Co, 5.8; C, 53.18; N, 12.91; H, 4.22.

Caution. Perchlorate salts with organic ligands are potentially explosive and should be handled with the necessary precautions.²⁴

Crystal Structure Determinations of $[\text{Co}_2(6\text{-bismbmp})_3](\text{ClO}_4)_4(\text{CH}_3\text{CN})_{2.5}$ (6**) and $[\text{Co}_2(5\text{-bismbmp})_3](\text{ClO}_4)_4(\text{CH}_3\text{CN})_6$ (**7**).** The determination of the crystal structures of compounds **6** and **7** presented a number of practical difficulties. The crystals are not easy to grow and lose solvent and disintegrate upon exposure to air. Crystals were therefore taken from the solution without drying and were sealed in capillary tubes with some mother liquor. Crystal data and details of intensity measurements and structure refinements are given in Table 1. Cell dimensions and intensities were measured at room temperature on Enraf-Nonius CAD 4 (**6**) and Philips PW1100 (**7**) diffractometers. Data were corrected for Lorentz and polarization but not for absorption effects ($\mu r < 0.2$). The structures were solved by direct methods using MULTAN 87;²⁵ all other calculations used XTAL²⁶ system and ORTEP II²⁷ programs. Atomic

(23) Büyüç, G.; Hardegger, E. *Helv. Chim. Acta* **1975**, *58*, 682–687.

(24) Wolsey, W. C. *J. Chem. Educ.* **1978**, *55*, A355.

(25) Main, P.; Fiske, S. J.; Hull, S. E.; Lessinger, L.; Germain, D.; Declercq, J. P.; Woolfson, M. M. MULTAN 87. Universities of York, England, and Louvaine-La-Neuve, Belgium, 1987.

(26) Hall, S. R.; Stewart, J. M., Eds. XTAL 3.0 User's Manual. Universities of Western Australia and Maryland, 1989.

(27) Johnson, C. K. ORTEP II; Report ORNL-5138; Oak Ridge National Laboratory: Oak Ridge, TN, 1976.

(20) Williams, A. F.; Piquet, C.; Bernardinelli, G. *Angew. Chem., Int. Ed. Engl.* **1991**, *30*, 1490–1492.

(21) Cotton, F. A.; Wilkinson, G. *Advanced Inorganic Chemistry*, 5th ed.; John Wiley: New York, Chichester, Brisbane, Toronto, Singapore, 1988; p 732.

(22) Purcell, K. F.; Kotz, J. C. *Inorganic Chemistry*; W. B. Saunders Co.: Philadelphia, London, Toronto, 1977; p 716.

Table 1. Summary of Crystal Data, Intensity Measurements, and Structure Refinement for $[\text{Co}_2(6\text{-bismbmp})_3](\text{ClO}_4)_4(\text{CH}_3\text{CN})_{2.5}$ (6) and $[\text{Co}_2(5\text{-bismbmp})_3](\text{ClO}_4)_4(\text{CH}_3\text{CN})_6$ (7)

	compd	
	6	7
formula	$\text{Co}_2(\text{C}_{29}\text{H}_{26}\text{N}_6)_3(\text{ClO}_4)_4(\text{CH}_3\text{CN})_{2.5}$	$\text{Co}_2(\text{C}_{29}\text{H}_{26}\text{N}_6)_3(\text{ClO}_4)_4(\text{CH}_3\text{CN})_6$
mol wt	1994.0	2137.7
cryst system	triclinic	triclinic
space group	$P\bar{1}$	$P\bar{1}$
<i>a</i> , Å	14.403(2)	13.648(5)
<i>b</i> , Å	16.558(3)	16.917(4)
<i>c</i> , Å	21.328(3)	22.801(8)
α , deg	78.15(1)	92.45(1)
β , deg	81.19(1)	103.80(1)
γ , deg	89.02(1)	96.32(1)
<i>V</i> , Å ³	4919(1)	5068(3)
<i>Z</i>	2	2
<i>D</i> _{calc} , g cm ⁻³	1.35	1.40
μ , mm ⁻¹	0.515	0.506
<i>R</i> , <i>R</i> _w ^a	0.110, 0.097	0.111, 0.111

^a $R = \sum ||F_o| - |F_c|| / \sum |F_o|$. ^b $R_w = [\sum w(|F_o| - |F_c|)^2 / \sum w|F_o|^2]^{0.5}$; $w = 1/\sigma^2(F_o)$.

scattering factors and anomalous dispersion terms were taken from ref 28. All coordinates of hydrogen atoms were calculated.

Both structures contain large cations (107 non-hydrogen atoms) between which are packed much smaller perchlorate anions and solvent molecules which are more or less disordered. The disorder results in high overall temperature factors and a rapid decrease in intensity of reflections as θ increases, limiting the number of observable reflections. In consequence it is not possible to model accurately the anions and the solvent molecules, and this results in rather high residual *R* factors as frequently observed in other structural determinations involving this type of compound.^{2b,12,13b,36}

For 6, three of the perchlorate molecules were relatively well ordered while the fourth showed five sites for the oxygen atoms, two of which were given population parameters of 0.5. Five acetonitrile molecules were located and were given population parameters of 0.5. Full-matrix block refinement was performed successively on ligand a and the cobalt atoms, ligand b, ligand c, and perchlorates and solvent molecules (maximum number of variables per block = 335, total number of parameters = 1151) using weights $1/\sigma^2(F_o)$. Anisotropic atomic displacement parameters were used for cobalt, chlorine, nitrogen, and ligand carbon atoms. Isotropic atomic displacement parameters were used for solvent carbon atoms and perchlorate oxygens.

For 7, all four perchlorate anions were disordered: two perchlorate anions were refined with six atomic positions for the oxygen atoms, one perchlorate was refined with seven sites for the oxygen atoms, and the last perchlorate was refined with two different atomic positions for the chlorine atoms associated respectively with five and seven positions for the oxygen atoms (for site occupancy factors, see Table SI). Of the six solvent molecules in 7, two were observed with three atomic sites, one with two atomic sites, and three with only one atomic site attributed to nitrogen atoms. Full-matrix refinement was performed using anisotropic atomic displacement parameters for cobalt, chlorine, and non-hydrogen ligand atoms. Isotropic atomic displacement parameters were used for solvent atoms and perchlorate oxygens. The greater disorder of the perchlorates and the solvent molecules in 7 led to physically unreasonable anisotropic atomic displacement parameters if weights $1/\sigma^2(F_o)$ were used, and unit weights were therefore applied.

Spectroscopic and Analytical Measurements. Electronic spectra in the UV-visible range were recorded in solution with Perkin-Elmer Lambda 5 and Lambda 2 spectrophotometers at 20 °C using quartz cells of 1, 0.1, and 0.01 cm path length. Spectrophotometric titrations were performed with a Perkin-Elmer Lambda 5 spectrophotometer connected to a personal computer. In a typical experiment, 50 mL of ligand 6-bismbmp (1) or 5-bismbmp (2) in acetonitrile (2×10^{-5} M) was titrated with a 2.2×10^{-4} M solution of $\text{Co}(\text{ClO}_4)_2 \cdot 6\text{H}_2\text{O}$ in acetonitrile. After each addition of 0.20 mL, the absorbances at 10 different wavelengths were recorded using a 1-cm quartz cell and transferred to the computer. Plots of extinction as a function of the metal/ligand ratio gave a first indication

of the number and stoichiometry of the complexes formed: factor analysis²⁹ was then applied to the data to confirm the number of different absorbing species. Finally, a model for the distribution of species was fitted with a nonlinear least-squares algorithm to give stability constants as previously described.^{18,30} IR spectra were obtained from KBr pellets with a Perkin-Elmer IR 883 spectrophotometer. ¹H-NMR and ¹³C-NMR spectra were recorded on Varian XL 200 and Bruker AMX 400 spectrometers. Chemical shifts are given in ppm with respect to TMS. Abbreviations: s, singlet; d, doublet; t, triplet; quart, quartet; m, multiplet. EI-MS (70 eV) were recorded with VG 7000E and Finnigan 4000 instruments. ES-MS (electron-spray/mass spectrometry) were recorded at the Laboratory of Mass Spectroscopy of Prof. J. D. Henion (Cornell University). Cyclic voltammograms were recorded using a Cypress System potentiostat connected to an ATM A386SX personal computer. A 3-electrode system consisting of a stationary Pt disk working electrode, a Pt counter electrode, and a nonaqueous Ag/Ag⁺ reference electrode was used. NBu_4PF_6 (0.1 M in CH_3CN) served as an inert electrolyte, and CH_3CN was distilled from P_2O_5 and then passed through an Alox column (activity I). The reference potential ($E^\circ = 0.37$ V vs SCE) was standardized against the known complex $[\text{Ru}(\text{bipy})_3](\text{ClO}_4)_2$.³¹ The scan speed used was 0.2 V/s, and voltammograms were analyzed according to established procedures.³¹ Coulometry at controlled potential was performed using the same equipment but with a 1-cm² Pt working electrode. Elemental analyses were performed by Dr. H. Eder of the Microchemical Laboratory of the University of Geneva. Metal contents were determined by atomic absorption (Pye Unicam SP9) after acidic oxidative mineralization of the complexes.

Results

Preparation of the Ligands. The bis-bidentate ligand bis[5-(1-methyl-2-(5'-methyl-2'-pyridyl)benzimidazolyl)]methane (5-bismbmp, 2) is prepared according to a convergent strategy based on a modified double Philips reaction³² as previously reported for the synthesis of bis[5-(1-methyl-2-(6'-methyl-2'-pyridyl)benzimidazolyl)]methane (6-bismbmp, 1)¹⁸ (Scheme 1). For unknown reasons, we were unable to synthesize the required 2-carboxy-5-methylpyridine (4) in one step from 2,5-lutidine.³³ In agreement with a literature report,²³ the oxidation of 2,5-lutidine with selenium dioxide gives 2-carboxy-5-methylpyridinium hydrogen selenite in satisfactory yield with only traces of the desired acid 4. However, the modification proposed by Büyükk and Hardegger²³ did not improve the yield in our hands, and we transformed the crude oxidized product to the ethyl ester (3) which was easily purified by distillation and then hydrolyzed to give the desired pure 2-carboxy-5-methylpyridine (4). A double Philips condensation of 4 with (3,3'-diamino-4,4'-bis(*N*-methylamino)-diphenyl)methane (5) under fused salt conditions¹⁸ gave a good yield of 5-bismbmp (2) after careful chromatography of the crude reaction product.

Preparation of Cobalt(II) Complexes. The Co(II) complexes are prepared by mixing ligands 6-bismbmp (1) or 5-bismbmp (2) with stoichiometric quantities of $\text{Co}(\text{H}_2\text{O})_6(\text{ClO}_4)_2$ in acetonitrile/dichloromethane. The perchlorate salts of the Co(II) complexes are obtained by slow evaporation of an acetonitrile solution at 60 °C for 6-bismbmp or by slow diffusion of methanol into a concentrated acetonitrile solution for 5-bismbmp. We obtain salmon colored crystals of $[\text{Co}_2(6\text{-bismbmp})_3](\text{ClO}_4)_4 \cdot 3\text{H}_2\text{O}$ and orange yellow prisms of $[\text{Co}_2(5\text{-bismbmp})_3](\text{ClO}_4)_4 \cdot 4\text{H}_2\text{O}$ whose elemental analyses after drying are compatible with these formulations. ES-MS spectra of both complexes from acetonitrile solutions show a single peak at $m/z = 373.2$ whose isotopic pattern

(29) Malinowski, E. R.; Howery, D. G. *Factor Analysis in Chemistry*; J. Wiley: New York, Chichester, Brisbane, Toronto, 1980.

(30) Gamp, H.; Maeder, M.; Meyer, C. J.; Zuberbühler, A. D. *Talanta* **1985**, *32*, 95–101.

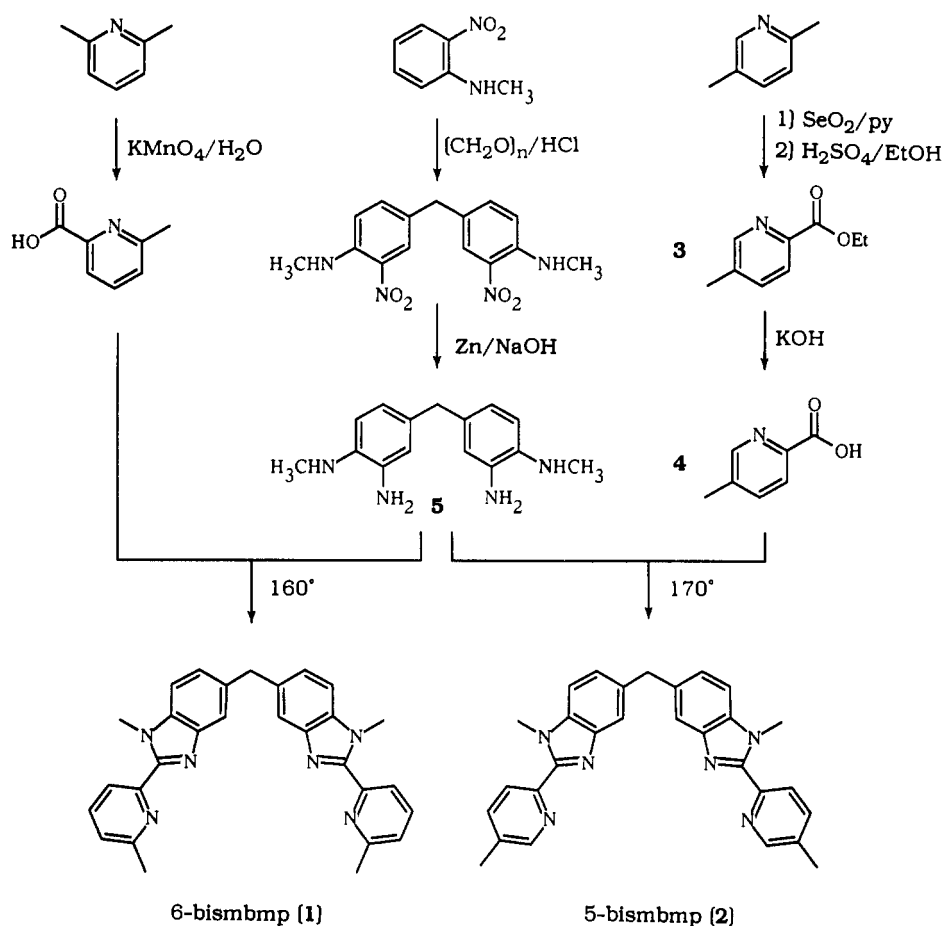
(31) Bard, A. J.; Faulkner, L. R. *Electrochemical Methods, Fundamentals and Application*; J. Wiley: New York, Chichester, Brisbane, Toronto, Singapore, 1980.

(32) Addison, A. W.; Burke, P. J. *J. Heterocycl. Chem.* **1981**, *18*, 803–805. Addison, A. W.; Rao, T. N.; Wahlgren, C. G. *J. Heterocycl. Chem.* **1983**, *20*, 1481–1484.

(33) Jerchel, D.; Heider, J.; Wagner, H. *Liebigs Ann. Chem.* **1958**, *613*, 153–170.

(28) *International Tables for X-ray Crystallography*; Kynoch Press: Birmingham, England, 1974; Vol. IV.

Scheme 1



corresponds to the cations $[\text{Co}_2(6\text{-bisbmbmp})_3]^{4+}$ and $[\text{Co}_2(5\text{-bisbmbmp})_3]^{4+}$. The IR spectra of complexes $[\text{Co}_2(6\text{-bisbmbmp})_3](\text{ClO}_4)_4 \cdot 3\text{H}_2\text{O}$ and $[\text{Co}_2(5\text{-bisbmbmp})_3](\text{ClO}_4)_4 \cdot 4\text{H}_2\text{O}$ are very similar and show the characteristic splitting of the ligand vibration at 1575 cm^{-1} ($\text{C}=\text{C}$, $\text{C}=\text{N}$ stretching) into two components at 1570 and 1605 cm^{-1} upon complexation to Co(II) .^{18,34} The ClO_4^- anions all show the two expected symmetrical vibrations (1095 , 625 cm^{-1}) typical of ionic perchlorates.³⁵

X-ray Crystal Structure of $[\text{Co}_2(6\text{-bisbmbmp})_3](\text{ClO}_4)_4(\text{CH}_3\text{CN})_{2,5}$ (6) and $[\text{Co}_2(5\text{-bisbmbmp})_3](\text{ClO}_4)_4(\text{CH}_3\text{CN})_6$ (7). Atomic coordinates are given in Tables 2 and 3; selected bond lengths and angles are in Table 4. Figure 1 shows the atomic numbering scheme, and Figures 2 and 3 give ORTEP²⁷ stereoscopic views of the complexes 6 and 7 perpendicular to the pseudo- C_3 axis.

In agreement with ES-MS and IR results, the crystal structures show 6 and 7 to be composed of the cations $[\text{Co}_2(6\text{-bisbmbmp})_3]^{4+}$ and $[\text{Co}_2(5\text{-bisbmbmp})_3]^{4+}$, respectively, four uncoordinated perchlorate anions, and solvent molecules. The anions and solvent molecules are more or less disordered (see Experimental Section) but otherwise show no features of interest. The dinuclear cations $[\text{Co}_2(6\text{-bisbmbmp})_3]^{4+}$ and $[\text{Co}_2(5\text{-bisbmbmp})_3]^{4+}$ adopt triple-helical structures where the three bis-bidentate ligands are wrapped around a pseudo- C_3 axis passing through the cobalt atoms. The aromatic rings of the ligands are planar within experimental error, and the helical twisting of the ligands 1 and 2 is achieved by twisting about the interannular $\text{C}-\text{C}$ bonds as previously reported for double-helical complexes with polypyridines.⁷ As observed³⁶ for the dinuclear triple-helical complex

$[\text{Eu}_2(\text{bisbmbzimpy})_3]^{6+}$, the main torsion responsible for the helical twist in 6 and 7 is found between the benzimidazole rings connected by the CH_2 bridge ($76.3\text{--}89.9^\circ$; see Table SIII), but we do not observe significant intramolecular stacking interactions between the different strands in 6 and 7. The coordination sites of the two cobalt atoms are very similar leading to a pseudo- D_3 symmetry for the dinuclear triple-helical cations. As a result of the small bite angles $\text{N}(\text{bzim})-\text{Co}-\text{N}(\text{py})$ within each chelate 2-(2'-benzimidazolyl)pyridine unit ($76(2)^\circ$ for 6 and 7), the coordination spheres around the cobalt atoms may be best described as octahedra flattened along the C_3 axis as found in the crystal structure of $[\text{Co}(\text{bipy})_3]^{2+}$ (average bite angle = $76(1)^\circ$)³⁷ (Figure 4).

To quantify this distortion and to facilitate comparison of 6 and 7, the coordination sphere around Co(II) has been investigated using a geometrical analysis assuming that C_3 symmetry is maintained (Scheme 2). Each pseudo-octahedron around the cobalt atoms is considered to be made up of two tripods defined by the $\text{Co}-\text{N}$ vectors related by pseudo- C_3 symmetry (one tripod with three pyridine nitrogen atoms (e.g. $\text{N}(3\text{a})$, $\text{N}(3\text{b})$, $\text{N}(3\text{c})$) and the other with three benzimidazole nitrogen atoms (e.g. $\text{N}(1\text{a})$, $\text{N}(1\text{b})$, $\text{N}(1\text{c})$); Scheme II). In the first part of the analysis, the sum vectors $\text{R}_1 = \text{Co}-\text{N}(3\text{a}) + \text{Co}-\text{N}(3\text{b}) + \text{Co}-\text{N}(3\text{c})$ and $\text{R}_2 = \text{Co}-\text{N}(1\text{a}) + \text{Co}-\text{N}(1\text{b}) + \text{Co}-\text{N}(1\text{c})$ are calculated together with the angle ϕ between them which measures the average bending of the two tripods connected to one cobalt atom. The angles θ_i between the sum vectors R_1 and the $\text{Co}-\text{N}(\text{py})$ vectors (or R_2 and $\text{Co}-\text{N}(\text{bzim})$) allow the quantitative determination of the flattening of the pseudo-octahedron along the C_3 axis.

(34) Piguet, C.; Bocquet, B.; Müller, E.; Williams, A. F. *Helv. Chim. Acta* **1989**, *72*, 323–337.

(35) Nakamoto, K. *Infrared and Raman Spectra of Inorganic and Coordination Compounds*, 3rd ed.; John Wiley: New York, Chichester, Brisbane, Toronto, 1972; pp 142–154.

(36) Bernardinelli, G.; Piguet, C.; Williams, A. F. *Angew. Chem., Int. Ed. Engl.* **1992**, *31*, 1622–1624. Piguet, C.; Bünzli, J.-C. G.; Bernardinelli, G.; Hopfgartner, G.; Williams, A. F. *J. Am. Chem. Soc.* **1993**, *115*, 8197–8206.

Table 2. Fractional Atomic Coordinates with Esd's in Parentheses, Atomic Displacement Parameters (\AA^2), and Population Parameters (PP (If $\neq 1$)) for $[\text{Co}_2(6\text{-bismbmp})_3](\text{ClO}_4)_4(\text{CH}_3\text{CN})_{2.5}$ (6)

	<i>x/a</i>	<i>y/b</i>	<i>z/c</i>	<i>U</i> _{eq} ^a	PP		<i>x/a</i>	<i>y/b</i>	<i>z/c</i>	<i>U</i> _{eq} ^a	PP
Co(1)	0.7430(2)	0.7443(1)	0.9650(1)	0.045(1)		N(1c)	0.669(1)	0.645(1)	0.9532(8)	0.047(8)	
Co(2)	0.7226(2)	0.7213(1)	0.5763(1)	0.041(1)		N(2c)	0.654(1)	0.508(1)	0.9655(9)	0.060(9)	
N(1a)	0.682(1)	0.8354(9)	0.9028(8)	0.043(8)		N(3c)	0.802(1)	0.632(1)	1.0274(9)	0.061(9)	
N(2a)	0.574(1)	0.930(1)	0.888(1)	0.07(1)		N(4c)	0.653(1)	0.810(1)	0.6183(9)	0.042(8)	
N(3a)	0.605(1)	0.765(1)	1.028(1)	0.055(9)		N(5c)	0.621(1)	0.943(1)	0.618(1)	0.054(9)	
N(4a)	0.848(1)	0.719(1)	0.6148(6)	0.038(7)		N(6c)	0.782(1)	0.840(1)	0.5123(8)	0.045(8)	
N(5a)	0.994(1)	0.675(1)	0.6227(7)	0.051(8)		C(1e)	0.596(2)	0.627(1)	0.9200(9)	0.04(1)	
N(6a)	0.814(1)	0.613(1)	0.5391(8)	0.051(8)		C(2e)	0.543(1)	0.682(1)	0.881(1)	0.043(9)	
C(1a)	0.714(2)	0.895(1)	0.845(1)	0.04(1)		C(3e)	0.477(2)	0.650(1)	0.8547(9)	0.05(1)	
C(2a)	0.794(1)	0.897(1)	0.801(1)	0.037(9)		C(4e)	0.465(1)	0.565(2)	0.863(1)	0.06(1)	
C(3a)	0.808(1)	0.963(1)	0.7507(9)	0.039(9)		C(5e)	0.520(2)	0.509(1)	0.898(1)	0.07(1)	
C(4a)	0.740(2)	1.022(1)	0.741(1)	0.07(1)		C(6e)	0.588(2)	0.542(1)	0.926(1)	0.05(1)	
C(5a)	0.659(2)	1.022(1)	0.784(1)	0.09(1)		C(7e)	0.701(2)	0.574(2)	0.979(1)	0.05(1)	
C(6a)	0.646(2)	0.955(1)	0.835(1)	0.06(1)		C(8e)	0.782(2)	0.563(2)	1.013(1)	0.05(1)	
C(7a)	0.599(2)	0.858(1)	0.929(1)	0.05(1)		C(9e)	0.833(2)	0.492(2)	1.026(1)	0.09(1)	
C(8a)	0.546(2)	0.814(1)	0.993(1)	0.06(1)		C(10c)	0.908(3)	0.492(2)	1.054(2)	0.14(2)	
C(9a)	0.447(2)	0.817(1)	1.009(1)	0.07(1)		C(11c)	0.927(2)	0.559(2)	1.075(1)	0.10(1)	
C(10a)	0.413(2)	0.771(2)	1.066(2)	0.09(1)		C(12c)	0.872(2)	0.632(2)	1.062(1)	0.09(1)	
C(11a)	0.471(2)	0.727(2)	1.106(1)	0.09(1)		C(13c)	0.411(1)	0.705(1)	0.816(1)	0.06(1)	
C(12a)	0.565(2)	0.726(1)	1.085(1)	0.06(1)		C(14c)	0.580(1)	0.815(1)	0.669(1)	0.03(1)	
C(13a)	0.899(1)	0.971(1)	0.7034(8)	0.056(9)		C(15c)	0.536(1)	0.751(1)	0.716(1)	0.034(9)	
C(14a)	0.891(1)	0.776(1)	0.6417(9)	0.04(1)		C(16c)	0.466(1)	0.772(1)	0.763(1)	0.04(1)	
C(15a)	0.864(1)	0.848(1)	0.6613(8)	0.039(8)		C(17c)	0.446(1)	0.855(1)	0.7627(9)	0.05(1)	
C(16a)	0.929(2)	0.893(1)	0.6831(8)	0.038(9)		C(18c)	0.491(1)	0.920(1)	0.717(1)	0.06(1)	
C(17a)	1.019(2)	0.866(1)	0.6847(9)	0.06(1)		C(19c)	0.561(2)	0.898(2)	0.668(1)	0.05(1)	
C(18a)	1.049(1)	0.794(2)	0.6670(9)	0.06(1)		C(20c)	0.672(1)	0.885(2)	0.590(1)	0.04(1)	
C(19a)	0.982(2)	0.748(1)	0.6458(8)	0.04(1)		C(21c)	0.751(2)	0.903(1)	0.537(1)	0.04(1)	
C(20a)	0.913(2)	0.662(1)	0.6040(9)	0.05(1)		C(22c)	0.794(2)	0.980(2)	0.519(1)	0.06(1)	
C(21a)	0.882(2)	0.595(1)	0.578(1)	0.05(1)		C(23c)	0.872(2)	0.990(1)	0.473(1)	0.09(1)	
C(22a)	0.918(1)	0.516(2)	0.5912(9)	0.07(1)		C(24c)	0.902(1)	0.927(2)	0.445(1)	0.08(1)	
C(23a)	0.884(2)	0.453(1)	0.566(1)	0.09(1)		C(25c)	0.859(2)	0.846(1)	0.465(1)	0.06(1)	
C(24a)	0.821(2)	0.472(2)	0.525(1)	0.08(1)		C(26c)	0.659(1)	0.417(1)	0.9866(9)	0.08(1)	
C(25a)	0.785(1)	0.550(2)	0.512(1)	0.07(1)		C(27c)	0.894(1)	0.708(2)	1.082(1)	0.11(1)	
C(26a)	0.486(2)	0.979(1)	0.901(1)	0.12(1)		C(28c)	0.610(1)	1.032(1)	0.6003(9)	0.07(1)	
C(27a)	0.628(1)	0.674(1)	1.1268(9)	0.07(1)		C(29c)	0.887(1)	0.775(1)	0.4370(9)	0.056(9)	
C(28a)	1.080(1)	0.628(1)	0.6138(8)	0.052(9)		Cl(1)	0.7114(4)	0.4419(5)	0.2793(3)	0.097(4)	
C(29a)	0.720(1)	0.572(1)	0.464(1)	0.08(1)		O(1)	0.611(1)	0.4381(9)	0.2819(7)	0.118(5)	
N(1b)	0.860(1)	0.729(1)	0.8982(7)	0.047(8)		O(2)	0.743(1)	0.359(1)	0.2890(8)	0.143(7)	
N(2b)	1.011(1)	0.756(1)	0.8581(9)	0.06(1)		O(3)	0.758(1)	0.490(1)	0.219(1)	0.178(8)	
N(3b)	0.842(1)	0.846(1)	0.968(1)	0.060(9)		O(4)	0.731(1)	0.4756(9)	0.3327(8)	0.114(5)	
N(4b)	0.659(1)	0.6178(8)	0.6412(8)	0.039(7)		Cl(2)	0.4625(6)	0.1934(4)	-0.2617(4)	0.110(4)	
N(5b)	0.576(1)	0.503(1)	0.6467(9)	0.049(9)		O(5)	0.480(1)	0.131(1)	-0.2961(8)	0.136(6)	
N(6b)	0.593(1)	0.701(1)	0.5331(9)	0.046(8)		O(6)	0.545(2)	0.221(1)	-0.244(1)	0.23(1)	
C(1b)	0.892(2)	0.669(2)	0.863(1)	0.05(1)		O(7)	0.417(1)	0.256(1)	-0.295(1)	0.176(8)	
C(2b)	0.845(1)	0.601(1)	0.8513(9)	0.044(9)		O(8)	0.413(2)	0.163(2)	-0.201(1)	0.28(1)	
C(3b)	0.901(2)	0.550(1)	0.815(1)	0.05(1)		Cl(3)	0.1758(6)	0.7895(4)	0.4523(4)	0.112(4)	
C(4b)	0.998(2)	0.569(2)	0.791(1)	0.07(1)		O(9)	0.158(1)	0.857(1)	0.410(1)	0.164(8)	
C(5b)	1.040(1)	0.638(2)	0.803(1)	0.07(1)		O(10)	0.225(2)	0.805(1)	0.499(1)	0.196(9)	
C(6b)	0.987(2)	0.686(2)	0.839(1)	0.05(1)		O(11)	0.109(2)	0.729(1)	0.467(1)	0.21(1)	
C(7b)	0.933(2)	0.780(2)	0.894(1)	0.06(1)		O(12)	0.245(3)	0.736(2)	0.426(2)	0.14(1)	0.50
C(8b)	0.920(2)	0.852(2)	0.921(1)	0.05(1)		O(12i)	0.107(4)	0.822(4)	0.501(3)	0.30(3)	0.50
C(9b)	0.972(2)	0.920(2)	0.901(1)	0.11(1)		Cl(4)	0.8402(6)	0.2472(5)	0.9805(5)	0.137(5)	
C(10b)	0.952(2)	0.989(2)	0.928(2)	0.14(2)		O(13)	0.898(1)	0.180(1)	0.9869(9)	0.154(7)	
C(11b)	0.875(2)	0.983(2)	0.976(2)	0.13(2)		O(14)	0.823(1)	0.279(1)	0.920(1)	0.161(8)	
C(12b)	0.825(2)	0.913(2)	0.993(1)	0.09(1)		O(15)	0.755(2)	0.230(1)	1.025(1)	0.179(9)	
C(13b)	0.860(2)	0.475(1)	0.8059(9)	0.07(1)		O(16)	0.895(1)	0.308(1)	1.005(1)	0.195(9)	
C(14b)	0.689(1)	0.554(1)	0.6863(9)	0.04(1)		N(10i)	0.932(2)	0.613(1)	0.316(1)	0.03(1)	0.50
C(15b)	0.758(1)	0.555(1)	0.725(1)	0.048(9)		C(10i)	0.875(2)	0.638(2)	0.297(1)	0.003(8)	0.50
C(16b)	0.781(2)	0.481(1)	0.765(1)	0.05(1)		C(10j)	0.798(2)	0.670(2)	0.273(1)	0.020(8)	0.50
C(17b)	0.723(2)	0.409(1)	0.766(1)	0.07(1)		N(20i)	0.670(2)	0.184(2)	0.379(1)	0.08(2)	0.50
C(18b)	0.653(2)	0.406(1)	0.728(1)	0.07(1)		C(20i)	0.640(3)	0.121(3)	0.400(2)	0.07(1)	0.50
C(19b)	0.639(1)	0.483(1)	0.689(1)	0.04(1)		C(20j)	0.604(3)	0.061(3)	0.426(2)	0.08(1)	0.50
C(20b)	0.591(1)	0.583(1)	0.619(1)	0.04(1)		N(30i)	-0.010(2)	0.849(2)	0.244(2)	0.07(2)	0.50
C(21b)	0.545(2)	0.633(1)	0.570(1)	0.05(1)		C(30i)	0.049(3)	0.815(2)	0.254(2)	0.04(1)	0.50
C(22b)	0.453(2)	0.614(1)	0.561(1)	0.06(1)		C(30j)	0.121(3)	0.764(3)	0.269(2)	0.09(1)	0.50
C(23b)	0.412(2)	0.667(2)	0.511(1)	0.08(1)		N(40i)	0.760(2)	-0.065(2)	0.288(2)	0.11(2)	0.50
C(24b)	0.465(2)	0.731(2)	0.475(1)	0.08(1)		C(40i)	0.777(3)	-0.012(3)	0.233(3)	0.08(1)	0.50
C(25b)	0.553(2)	0.748(1)	0.485(1)	0.06(1)		C(40j)	0.768(2)	0.019(2)	0.183(2)	0.07(1)	0.50
C(26b)	1.109(1)	0.789(1)	0.846(1)	0.10(1)		N(50i)	0.336(4)	0.965(4)	0.032(3)	0.32(5)	0.50
C(27b)	0.742(2)	0.907(1)	1.048(1)	0.12(1)		C(50i)	0.298(4)	0.941(3)	0.072(3)	0.11(2)	0.50
C(28b)	0.513(1)	0.443(1)	0.631(1)	0.08(1)		C(50j)	0.217(4)	0.887(4)	0.136(3)	0.19(3)	0.50
C(29b)	0.611(1)	0.818(1)	0.444(1)	0.08(1)							

^a *U*_{eq} is the average of eigenvalues of *U*.

Finally, we have calculated the projections of the cobalt and the six nitrogen atoms of the coordination sphere onto a plane

perpendicular to the R_1 – R_2 direction. The angles ω_i between the vectors $\text{Co-proj}[N(i)]$ belonging to the same ligand show the

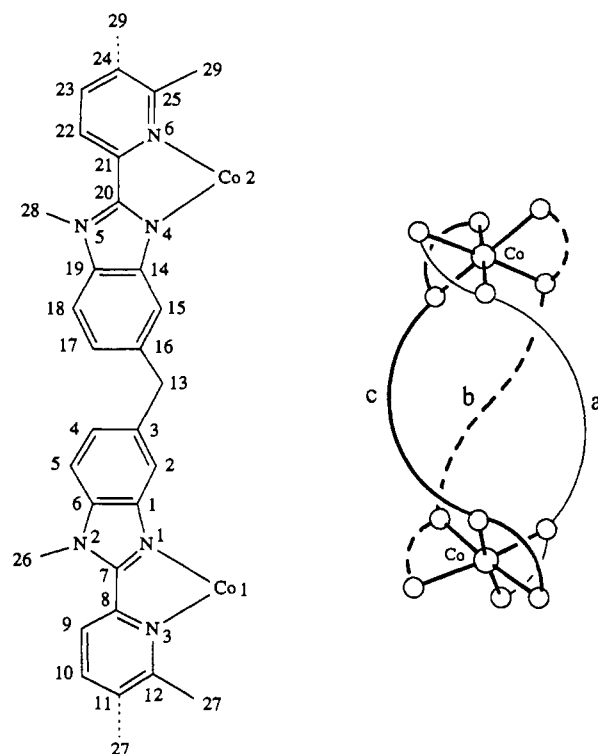
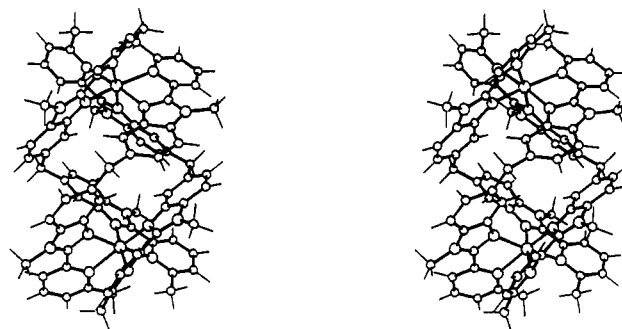
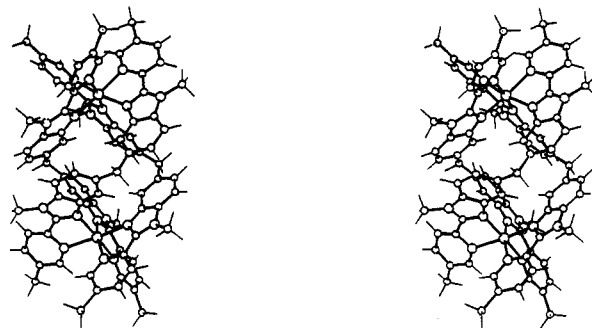
Table 4. Selected Bond Distances (Å) and Angles (deg) for $[\text{Co}_2(6\text{-bismbmp})_3](\text{ClO}_4)_4(\text{CH}_3\text{CN})_{2.5}$ (**6**) and $[\text{Co}_2(5\text{-bismbmp})_3](\text{ClO}_4)_4(\text{CH}_3\text{CN})_6$ (**7**)

		Distances	
		6	7
Co(1)–Co(2)	Co–Co	8.427(4)	8.854(4)
Co(1)–N(3a)	Co–N(py) ^a	2.29(2)	2.15(2)
Co(1)–N(3b)		2.24(2)	2.19(2)
Co(1)–N(3c)		2.28(2)	2.16(2)
Co(2)–N(6a)		2.40(2)	2.17(2)
Co(2)–N(6b)		2.26(2)	2.20(2)
Co(2)–N(6c)		2.25(1)	2.16(2)
Co(1)–N(1a)	Co–N(bzim)	2.07(2)	2.07(2)
Co(1)–N(1b)		2.08(2)	2.09(2)
Co(1)–N(1c)		2.05(2)	2.12(2)
Co(2)–N(4a)		2.09(2)	2.11(2)
Co(2)–N(4b)		2.10(2)	2.12(2)
Co(2)–N(4c)		2.04(1)	2.11(2)
		Angles	
		6	7
N(py)–Co–N(bzim) "Bite Angles"			
N(1a)–Co(1)–N(3a)		78.4(7)	77.4(7)
N(1b)–Co(1)–N(3b)		75.9(7)	77.7(7)
N(1c)–Co(1)–N(3c)		74.7(7)	76.5(7)
N(4a)–Co(2)–N(6a)		74.0(6)	76.6(7)
N(4b)–Co(2)–N(6b)		77.3(6)	76.3(7)
N(4c)–Co(2)–N(6c)		76.7(6)	75.1(9)
N(py)–Co–N(py)			
N(3a)–Co(1)–N(3b)		106.9(7)	93.7(7)
N(3a)–Co(1)–N(3c)		102.2(7)	96.6(7)
N(3b)–Co(1)–N(3c)		102.7(7)	96.0(7)
N(6a)–Co(2)–N(6b)		96.9(7)	99.7(7)
N(6a)–Co(2)–N(6c)		105.9(6)	92.9(8)
N(6b)–Co(2)–N(6c)		102.2(6)	98.2(8)
N(bzim)–Co–N(bzim)			
N(1a)–Co(1)–N(1b)		95.9(6)	99.8(7)
N(1a)–Co(1)–N(1c)		98.2(7)	96.0(7)
N(1b)–Co(1)–N(1c)		95.2(7)	101.6(6)
N(4a)–Co(2)–N(4b)		97.3(6)	96.9(7)
N(4a)–Co(2)–N(4c)		99.5(7)	96.4(6)
N(4b)–Co(2)–N(4c)		97.7(6)	101.1(8)
N(py)–Co–N(bzim) "Trans"			
N(1a)–Co(1)–N(3c)		172.7(8)	170.8(7)
N(1b)–Co(1)–N(3a)		173.2(7)	170.9(7)
N(1c)–Co(1)–N(3b)		171.0(7)	172.5(7)
N(4a)–Co(2)–N(6b)		170.3(7)	172.3(7)
N(4b)–Co(2)–N(6c)		174.4(6)	173.5(8)
N(4c)–Co(2)–N(6a)		172.5(7)	166.4(9)
N(py)–Co–N(bzim) "Cis"			
N(1a)–Co(1)–N(3b)		84.0(7)	91.4(7)
N(1b)–Co(1)–N(3c)		83.0(6)	87.1(7)
N(1c)–Co(1)–N(3a)		82.1(7)	87.4(6)
N(4a)–Co(2)–N(6c)		84.0(6)	88.9(8)
N(4b)–Co(2)–N(6a)		79.7(5)	91.4(7)
N(4c)–Co(2)–N(6b)		89.2(7)	88.6(6)

deformation of the pseudo-octahedron ($\omega_i = 60^\circ$) toward a trigonal prism ($\omega_i = 0^\circ$). The values for ϕ , θ_i , and ω_i are reported in Table 5 for each pseudo-octahedron. An identical geometrical analysis was performed with the normalized vectors $\langle \text{Co-N} \rangle = \text{Co-N} / \sqrt{(\text{Co-N} \cdot \text{Co-N})}$, but the results were very close to those reported in Table 5 and were not considered further for the discussion.

For both **6** and **7**, the ϕ angles ($171\text{--}178^\circ$) deviate only slightly from the value expected for a perfect octahedron (180°) indicating only a small bending of the two tripods within each coordination sphere. This is confirmed by the almost parallel arrangement of the facial planes formed by the three nitrogen atoms of each tripod (interplane angles $1\text{--}5^\circ$; Table SIII).

The θ_i angles for **6** and **7** are systematically larger than 54.7° , the value expected for a perfect octahedron, which demonstrates

**Figure 1.** Atomic numbering scheme for $[\text{Co}_2(6\text{-bismbmp})_3](\text{ClO}_4)_4(\text{CH}_3\text{CN})_{2.5}$ (**6**) (full line) and $[\text{Co}_2(5\text{-bismbmp})_3](\text{ClO}_4)_4(\text{CH}_3\text{CN})_6$ (**7**) (dotted line).**Figure 2.** ORTEP²⁷ stereoscopic view of $[\text{Co}_2(6\text{-bismbmp})_3]^{4+}$ perpendicular to the pseudo- C_3 axis.**Figure 3.** ORTEP²⁷ stereoscopic view of $[\text{Co}_2(5\text{-bismbmp})_3]^{4+}$ perpendicular to the pseudo- C_3 axis.

the flattening along the pseudo- C_3 axis. For $[\text{Co}_2(5\text{-bismbmp})_3]^{4+}$, θ_i ($58\text{--}63^\circ$) do not significantly deviate from the average value $60(2)^\circ$ and we conclude that the flattening is very similar for the pyridine and the benzimidazole tripods. However, for $[\text{Co}_2(6\text{-bismbmp})_3]^{4+}$, the pyridine tripods are significantly more flattened ($\theta_i = 61\text{--}69^\circ$; average $65(2)^\circ$) than the benzimidazole tripods ($\theta_i = 58\text{--}62^\circ$; average $60(1)^\circ$), and this is confirmed by the N(py)–Co–N(py) angles ($96.9\text{--}106.9$; average $104(3)^\circ$) which are significantly larger than those found in $[\text{Co}_2(5\text{-bismbmp})_3]^{4+}$

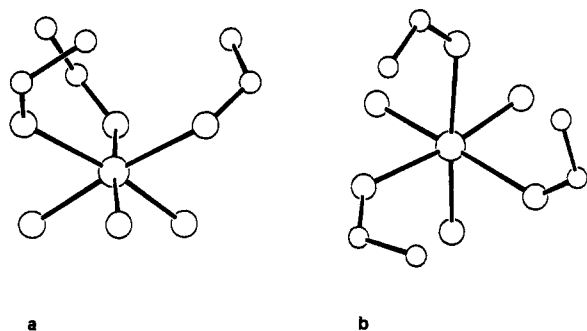
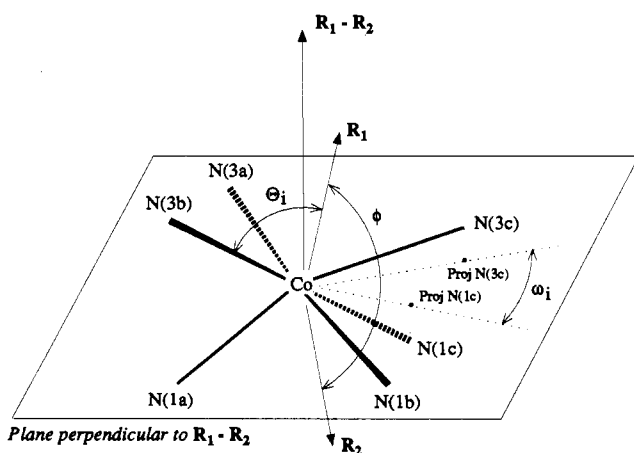


Figure 4. ORTEP²⁷ view of the coordination sphere of one of the cobalt ions in **6** showing the six coordinated nitrogens together with the carbon atoms of position 6 and of the attached methyl group: (a) perpendicular to the pseudo- C_3 axis showing the flattening; (b) along the C_3 axis showing short methyl-methyl distances.

Scheme 2



(95.2–99.5°; average 97(1)°) and for $[\text{Co}(\text{bipy})_3]^{2+}$ (92.4–96.1°; average 94(2)°).³⁷ We attribute this deformation to steric repulsions between the methyl groups bound to the 6-positions of the pyridine rings, since the distances between the carbon atoms of these methyls are quite short (average value 4.05(2) Å) (Figure 4). For a perfect octahedron the expected value of ω_i is 60°, but the observed values of 55(2)° for **6** and 51(2)° for **7** are slightly smaller implying a slight untwisting of the strands compared to a perfect octahedron, which we associate with the formation of the helix. The lower value for **7** is responsible for the longer Co–Co distance (8.854(4) Å) compared to **6** (8.427(4) Å). It is possible that methyl–methyl repulsion in **6** limits the extent to which the coordination sphere may untwist.

The Co–N(bzim) distances are slightly shorter in **6** (average 2.07(2) Å) than in **7** (average 2.11(3) Å), but both lie close to the standard value for Co(II)–imidazole bonds of 2.103 Å.³⁸ In **7**, where the interaction between the methyls is absent, the Co–N(py) distance (average 2.17(3)) is close to the standard value of 2.185 Å³⁸ and the 2.13(1) Å found in $[\text{Co}(\text{bipy})_3]^{2+}$.³⁷ In **6** however the Co–N(py) distances show considerable variation (2.24–2.40 Å) and the average value of 2.29(6) Å is much longer than that for **7**. The steric effect of the methyl groups in the 6 position is thus clearly shown by the bond distances. Finally, the two octahedra within each triple-helical cation adopt a slightly bent orientation as demonstrated by the dihedral angles between the facial planes (Table SIII) belonging to different coordination spheres (15(2)° for **6**; 25(1)° for **7**).

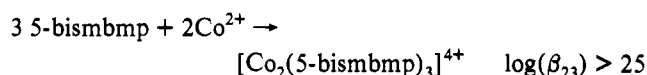
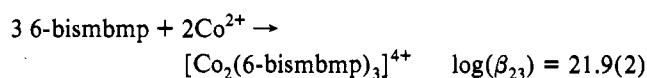
Structures and Properties in Solution. As reported for 6-bisbmbp (**1**),¹⁸ spectrophotometric titrations of 5-bisbmbp (**2**) with

Table 5. Structural Data (deg) for the Cobalt Coordination Spheres for $[\text{Co}_2(6\text{-bisbmbp})_3](\text{ClO}_4)_4(\text{CH}_3\text{CN})_{2.5}$ (**6**) and $[\text{Co}_2(5\text{-bisbmbp})_3](\text{ClO}_4)_4(\text{CH}_3\text{CN})_6$ (**7**) (py = Pyridine; bzim = Benzimidazole)

	6	7
Angles ϕ^a		
$R_1\text{-Co}(1)\text{-}R_2$	176	178
$R_1\text{-Co}(2)\text{-}R_2$	171	177
Angles (θ_i^b) for Tripod [N(py)–N(py)–N(py)]		
$R_1\text{-Co}(1)\text{-}N(3a)$	66	59
$R_1\text{-Co}(1)\text{-}N(3b)$	68	57
$R_1\text{-Co}(1)\text{-}N(3c)$	63	60
$R_1\text{-Co}(2)\text{-}N(6a)$	61	59
$R_1\text{-Co}(2)\text{-}N(6b)$	61	63
$R_1\text{-Co}(2)\text{-}N(6c)$	69	58
Angles θ_i for Tripod [N(bzim)–N(bzim)–N(bzim)]		
$R_2\text{-Co}(1)\text{-}N(1a)$	60	60
$R_2\text{-Co}(1)\text{-}N(1b)$	58	64
$R_2\text{-Co}(1)\text{-}N(1c)$	60	60
$R_2\text{-Co}(2)\text{-}N(4a)$	61	58
$R_2\text{-Co}(2)\text{-}N(4b)$	59	62
$R_2\text{-Co}(2)\text{-}N(4c)$	62	62
Angles ω_i^c		
proj[N(1a)]–Co(1)–proj[N(3a)] ^b	57	50
proj[N(1b)]–Co(1)–proj[N(3b)]	55	51
proj[N(1c)]–Co(1)–proj[N(3c)]	54	52
proj[N(4a)]–Co(1)–proj[N(6a)]	54	48
proj[N(4b)]–Co(1)–proj[N(6b)]	53	52
proj[N(4c)]–Co(1)–proj[N(6c)]	55	50

^a R_1 and R_2 are the vectors formed by summing the Co–N(py) and Co–N(bzim) vectors, respectively. For the definitions of ϕ , θ_i , and ω_i see text and Scheme 2. The error in the angles is typically 1°. ^b Proj[N(i)] is the projection of N(i) onto the plane perpendicular to $R_1\text{-}R_2$ and passing through the cobalt atom.

$\text{Co}(\text{H}_2\text{O})_6(\text{ClO}_4)_2$ in acetonitrile (Co:ligand ratio in the range 0.15–1.33) show a sharp end point near a Co:ligand ratio of 0.7. Isobestic points at 30 120 and 30 490 cm^{-1} are observed during the titration of 6-bisbmbp (**1**) and 5-bisbmbp (**2**) which imply the existence of only two absorbing species in solution for each titration. These results are confirmed by factor analysis,²⁹ and the spectrophotometric data can be satisfactorily fitted with a single equilibrium involving the dinuclear cations $[\text{Co}_2(6\text{-bisbmbp})_3]^{4+}$ and $[\text{Co}_2(5\text{-bisbmbp})_3]^{4+}$.



The stability constant for the formation of $[\text{Co}_2(6\text{-bisbmbp})_3]^{4+}$ is comparable to that found for the triple-helical complex $[\text{Eu}_2(\text{bisbmbp})_3]^{6+}$ under similar conditions ($\log(\beta_{23}) = 20.7(7)$).³⁶ With a total concentration of 1.89×10^{-5} M for 6-bisbmbp and 1.25×10^{-5} M for Co(II) (Co:ligand ratio = 0.67), the Bjerrum complex formation function³⁹ \bar{n} reaches a value of 1.15 which allows a rather accurate determination of the stability constant. However, for 5-bisbmbp in the same conditions, the \bar{n} value is close to 1.5 and consequently does not allow a precise determination of the stability constant which can only be estimated to be greater than 10^{25} .

The intense $\pi_1 \rightarrow \pi^*$ transitions of the ligand⁴⁰ (31 650 cm^{-1} and $\epsilon = 54\,250 \text{ M}^{-1} \text{ cm}^{-1}$ for 5-bisbmbp) do not change significantly upon complexation to Co(II) (Table 6), but two weak bands appear in the visible region. These bands are typical

(37) Szalda, D. J.; Creutz, C.; Mahajan, D.; Sutin, N. *Inorg. Chem.* **1983**, *22*, 2372–2379.

(38) Orpen, A. G.; Brammer, L.; Allen, F. H.; Kennard, O.; Watson, D. G.; Taylor, R. *J. Chem. Soc., Dalton Trans.* **1989**, S1–S83.

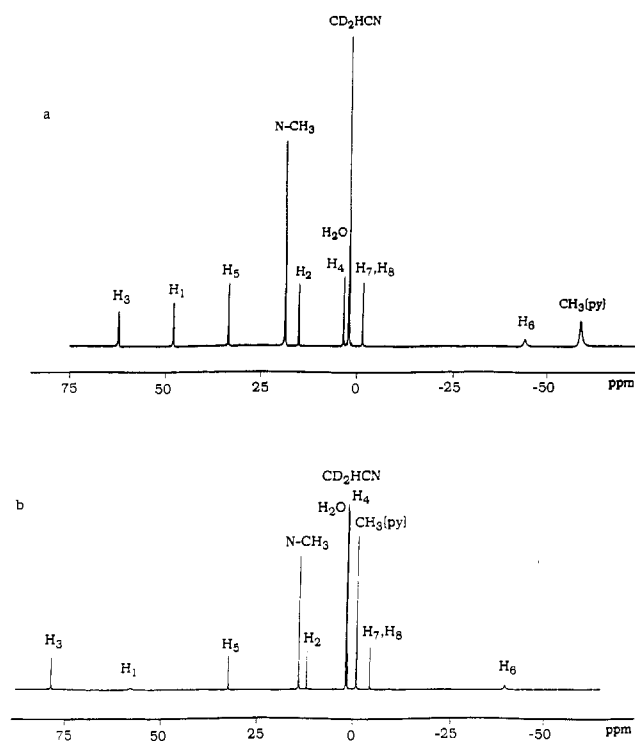
(39) Hartley, F. R.; Burgess, C.; Alcock, R. M. *Solution Equilibria*; Ellis Horwood Limited: Chichester, U.K., 1980; p 54.

(40) Nakamoto, K. *J. Phys. Chem.* **1960**, *64*, 1420–1425. Bray, R. G.; Ferguson, J.; Hawkins, C. J. *Aust. J. Chem.* **1969**, *22*, 2091–2103.

Table 6. Electronic Spectral Data for the Ligands 6-bisbmbp (1) and 5-bisbmbp (2) and Complexes $[\text{Co}_2(6\text{-bisbmbp})_3]^{4+}$ and $[\text{Co}_2(5\text{-bisbmbp})_3]^{4+}$ in CH_3CN^a and Electrochemical Reduction Potentials in $\text{CH}_3\text{CN} + 0.1 \text{ M NBu}_4\text{PF}_6^b$ at 20 °C

compd	$\pi_1 \rightarrow \pi^*$	d-d	$E_{1/2}$	$E_{pa} - E_{pc}$
6-bisbmbp	31 550 (46 800)		c	
5-bisbmbp	31 650 (54 250)		c	
$[\text{Co}_2(6\text{-bisbmbp})_3]^{4+}$	30 870 (111 930)	11 000 (8)	-1.05	90
		18 600 (67), sh	-1.25	240, irrev
		19 230 (79), sh		
		19 960 (93)		
$[\text{Co}_2(5\text{-bisbmbp})_3]^{4+}$	30 490 (129 000)	11 240 (9)	+0.37	160
		18 690 (40)	-1.19	90
			-1.68	530, irrev

^a Energies are given for the maximum of the band envelope in cm^{-1} , and ϵ (in parentheses), in $\text{M}^{-1} \text{cm}^{-1}$; sh = shoulder. ^b Electrochemical potentials are given in V vs SCE and $E_{pa} - E_{pc}$ in mV. Estimated error on $E_{1/2}$ is $\pm 0.01 \text{ V}$. ^c Too insoluble in $\text{CH}_3\text{CN} + 0.1 \text{ M NBu}_4\text{PF}_6$.

**Figure 5.** 200-MHz $^1\text{H-NMR}$ spectra of (a) $[\text{Co}_2(6\text{-bisbmbp})_3]^{4+}$ and (b) $[\text{Co}_2(5\text{-bisbmbp})_3]^{4+}$ in CD_3CN .

of d-d transitions for high-spin Co(II) in pseudo-octahedral environments.⁴¹ Assuming O_h microsymmetry, the low-energy transition (11 250–11 000 cm^{-1}) can be attributed to $^4\text{T}_{1g} \rightarrow ^4\text{T}_{2g}$ while the structured bands at higher energy (18 500–20 000 cm^{-1}) correspond to $^4\text{T}_{1g} \rightarrow ^4\text{T}_{1g}(\text{P})$ with admixture of spin-forbidden transitions derived from the ^2G and ^2H states. Unfortunately we were unable to observe the expected weak (formally two electron) $^4\text{T}_{1g} \rightarrow ^4\text{A}_{2g}$ transitions which would allow the calculation of $10Dq$ for both complexes.⁴¹ Nevertheless, the similarity of the d-d spectra indicates that similar octahedral high-spin $[\text{Co}^{\text{II}}\text{N}_6]^{2+}$ chromophores exist in both $[\text{Co}_2(6\text{-bisbmbp})_3]^{4+}$ and $[\text{Co}_2(5\text{-bisbmbp})_3]^{4+}$.

The $^1\text{H-NMR}$ spectra of the complexes $[\text{Co}_2(6\text{-bisbmbp})_3]^{4+}$ and $[\text{Co}_2(5\text{-bisbmbp})_3]^{4+}$ display seven singlets each with an integral of 1 and two singlets with an integral of 3 spread over more than 100 ppm (Figure 5). As a result of the contact and dipolar relaxation mechanisms arising from the coupling of

electronic and nuclear magnetic moments,⁴² the hyperfine structure is not observed in the one-dimensional spectra, but a detailed analysis of two-dimensional homonuclear $^1\text{H-}^1\text{H}$ and heteronuclear $^1\text{H-}^{13}\text{C}$ NMR correlation spectra allows the complete assignment of the nine signals (Table 7). Previous work on the $^1\text{H-NMR}$ spectra of $[\text{Co}_2(6\text{-bisbmbp})_3]^{4+}$ and analogous complexes showing the $^1\text{H-NMR}$ intramolecular diastereotopic effect^{16,18} has firmly established a pseudo- D_3 symmetry for the cation in solution in agreement with the crystal structure. The comparison of the $^1\text{H-NMR}$ spectra for both cations (Figure 5) clearly indicates that $[\text{Co}_2(5\text{-bisbmbp})_3]^{4+}$ also displays a pseudo- D_3 symmetry in acetonitrile solution. Surprisingly, the pyridine proton H_3 displays very different chemical shifts in the $^1\text{H-NMR}$ spectra of **6** and **7** (Table 7). Since the connectivities and the topologies of these protons are identical in $[\text{Co}_2(6\text{-bisbmbp})_3]^{4+}$ and $[\text{Co}_2(5\text{-bisbmbp})_3]^{4+}$, we can reasonably assume comparable Fermi contact shifts, and the variations observed in their chemical shifts probably arise from different dipolar contributions⁴² which suggest different structural orientations of the pyridine rings around Co(II) for $[\text{Co}_2(6\text{-bisbmbp})_3]^{4+}$ and $[\text{Co}_2(5\text{-bisbmbp})_3]^{4+}$ in agreement with the deformation of the coordination spheres observed in the X-ray crystal structures.

$[\text{Co}_2(6\text{-bisbmbp})_3]^{4+}$ is reduced on a platinum disk electrode in a quasi-reversible two-electron wave at $E_{1/2} = -1.05 \text{ V}$ vs SCE in $\text{MeCN} + 0.1 \text{ M NBu}_4\text{PF}_6$ (Co(II)/Co(I); $E^a - E^c = 90 \text{ mV}$) as well as in one irreversible wave at $E_{p/2} = -1.25 \text{ V}$. This second wave is attributed to ligand-based reductions⁴³ and is accompanied by deposition of electro-active material on the platinum electrode which is oxidized at -1.01 V (intense asymmetric peak in the cyclic voltammogram). This behavior parallels that of $[\text{Co}(\text{bipy})_3]^{2+}$ where a first reversible reduction wave, corresponding to Co(II)/Co(I), is observed at $E_{1/2} = -0.95 \text{ V}$, and a second irreversible reduction wave at more negative potential.⁴³ Similarly, $[\text{Co}_2(5\text{-bisbmbp})_3]^{4+}$ displays two successive reduction processes on a platinum disk electrode: a first quasi-reversible two electron wave at $E_{1/2} = -1.19 \text{ V}$ vs SCE in $\text{MeCN} + 0.1 \text{ M NBu}_4\text{PF}_6$ (Co(II)/Co(I); $E^a - E^c = 90 \text{ mV}$) followed by a second irreversible wave at $E_{p/2} = -1.68 \text{ V}$. Compared to $[\text{Co}_2(6\text{-bisbmbp})_3]^{4+}$, the reduction to Co(I) is less favorable for $[\text{Co}_2(5\text{-bisbmbp})_3]^{4+}$, but the most striking difference in the cyclic voltammograms of $[\text{Co}_2(6\text{-bisbmbp})_3]^{4+}$ and $[\text{Co}_2(5\text{-bisbmbp})_3]^{4+}$ concerns the oxidation processes centered on the metal. For $[\text{Co}_2(6\text{-bisbmbp})_3]^{4+}$ we do not observe any well-defined oxidation processes on a platinum disk electrode below $+1.6 \text{ V}$ vs SCE. For $[\text{Co}_2(5\text{-bisbmbp})_3]^{4+}$ a quasi-reversible wave is obtained at $E_{1/2} = +0.37 \text{ V}$ vs SCE in $\text{MeCN} + 0.1 \text{ M NBu}_4\text{PF}_6$ (Co(III)/Co(II); $E^a - E^c = 160 \text{ mV}$) which can be compared with the reversible wave of $[\text{Co}(\text{bipy})_3]^{3+/2+}$ ($E_{1/2} = +0.32 \text{ V}$ vs SCE).⁴³ Controlled-potential Coulometric experiments ($E = +0.8 \text{ V}$ vs SCE) show that 2.0(2) electrons per mole of complex are exchanged which could be in part responsible for the observed broadening of the oxidation wave⁴⁴ and strongly suggest the formation of yellow $[\text{Co}^{\text{III}}_2(5\text{-bisbmbp})_3]^{6+}$ in acetonitrile solution. The electronic spectrum of the oxidized solution shows a splitting of the $\pi_1 \rightarrow \pi^*$ band which is in agreement with the higher charge of the metal ion,³⁴ but unfortunately this intense absorption masks the region where the weak d-d transitions are expected.^{40,41} Varying the scan rate between 50 and 200 mV/s produced no significant modification of the oxidation or reduction waves. A detailed analysis of the shape of these waves according to Richardson and Taube⁴⁴ shows $E_p - E_{p/2}$ values around 50 mV leading to $\Delta E_{1/2} \approx 36 \text{ mV}$, typical of dinuclear complexes with

(41) Lever, A. B. P. *Inorganic Electronic Spectroscopy*, 2nd ed.; Studies in Physical and Theoretical Chemistry Vol. 33; Elsevier: New York, 1984; p 479.

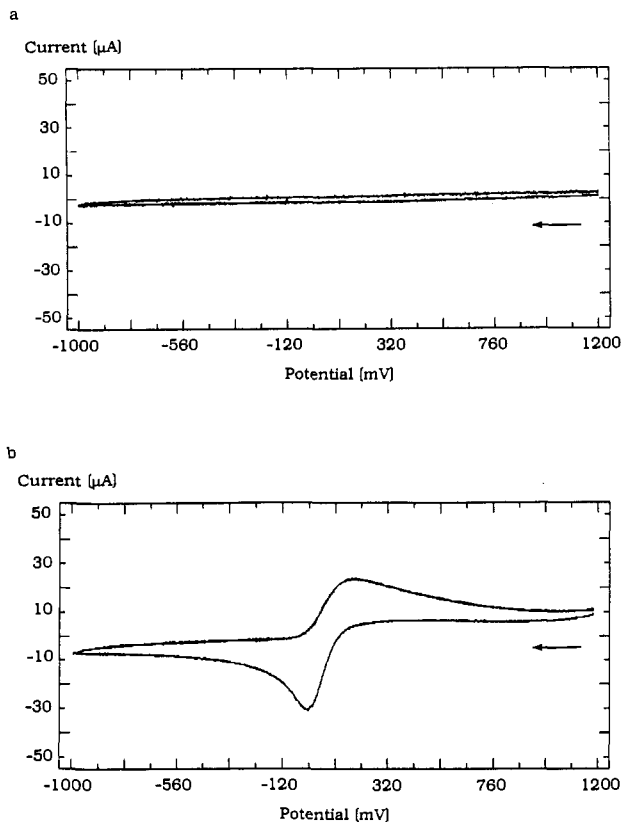
(42) Bertini, I.; Luchinat, C. *NMR of Paramagnetic Molecules in Biological Systems*; Benjamin/Cummings Publishing Co. Inc.: Menlo Park, CA, 1986.

(43) Margel, S.; Smith, W.; Anson, F. C. *J. Electrochem. Soc.* **1978**, *125*, 241–246.

(44) Richardson, D. E.; Taube, H. *Inorg. Chem.* **1981**, *20*, 1278–1285.

Table 7. ¹H-NMR Shifts (ppm, with respect to TMS) for Ligands 6-bisbmbp (**1**) and 5-bisbmbp (**2**) in CDCl₃ and [Co₂(6-bisbmbp)₃]⁴⁺ and [Co₂(5-bisbmbp)₃]⁴⁺ in CD₃CN

compd	H ₁	H ₂	H ₃	H ₄	H ₅	H ₆	H _{7,8}	py-CH ₃	N-CH ₃
6-bisbmbp (1)	7.16	7.69	8.14	7.30	7.19	7.68	4.26	2.61	4.23
5-bisbmbp (2)	8.50	7.64	8.25	7.30	7.20	7.68	4.27	2.39	4.22
[Co ₂ (1) ₃] ⁴⁺	47.6	15.1	62.2	3.6	33.1	-43.5	-1.5	-58.1	18.7
[Co ₂ (2) ₃] ⁴⁺	58.8	12.6	80.6	1.7	33.4	-40.2	-4.2	-0.7	14.8

**Figure 6.** Cyclic voltammograms on a platinum disk electrode ($v = 0.2$ V/s) for the oxidation processes Co(II)/Co(III) in (a) [Co₂(6-bisbmbp)₃]⁴⁺ and (b) [Co₂(5-bisbmbp)₃]⁴⁺ (CH₃CN + 0.1 M NBu₄PF₆). Potentials are given vs the Ag/Ag⁺ reference electrode.

weak interactions between metal sites.⁴⁵ This is not unexpected given the large Co-Co distances in these complexes.

Discussion

The structural analysis of the deviations from a perfect octahedral coordination leads to the identification of three factors. The first is a flattening of the octahedron along the C₃ axis, which is largely attributable to the bite angle of the chelate ligands being less than the ideal 90° and which for [Co₂(5-bisbmbp)₃]⁴⁺ is not greatly different from that observed for [Co(bipy)₃]²⁺. The second is the slight distortion of the coordination sphere toward a trigonal prism, shown by the ω_i values below 60°, which we attribute to constraints arising from the bridge between the two chelate units of the ligand, and the organization necessary for helix formation. Finally, in the case of [Co₂(6-bisbmbp)₃]⁴⁺, the methyl groups in the 6-position of the pyridine show sufficient interaction to produce a further distortion of the coordination sphere, resulting in lengthening of the Co-N(py) bond distances and a greater flattening of the octahedron but a diminution of the distortion toward a trigonal prism.

(45) De Santis, G.; Fabbrizzi, L.; Licchelli, M. P.; Pallavicini, P. *Coord. Chem. Rev.* **1992**, *120*, 237-257.

The spectroscopic titration and the ES-MS data show no evidence of intermediates in the formation of the complex in solution, implying that the process is probably a strict self-assembly as recently shown for double-helical complexes with Cu(I) or Ag(I).¹⁷ However, the additional distortion present in [Co₂(6-bisbmbp)₃]⁴⁺ strongly influences the properties in solution. The ¹H-NMR spectra of the two helices show differences, and the helix with 6-bisbmbp is less stable. The most spectacular difference is seen in the electrochemistry, the complex with 6-bisbmbp being slightly easier to reduce to cobalt(I) but impossible to oxidize to Co(III). The mononuclear complex [Co(bipy)₃]²⁺ may be oxidized to Co(III) or reduced to Co(I),⁴⁶ and structural data^{37,47,48} show that the oxidation is associated with a contraction of the Co-N bond distances of 0.19 Å while reduction results in a small elongation of 0.02 Å. The interactions between the methyls in [Co₂(6-bisbmbp)₃]⁴⁺ are such that the contraction of ≈0.19 Å required for oxidation to the low-spin Co(III) complex would be energetically expensive and no oxidation of the complex was observed, in contrast to the less sterically hindered [Co₂(5-bisbmbp)₃]⁴⁺. On the other hand, reduction to Co(I), and the associated lengthening of the Co-N bonds, would reduce the methyl-methyl repulsions, and this would explain the less negative reduction potential of [Co₂(6-bisbmbp)₃]⁴⁺.

Although the influence of methyl groups in the position α to a pyridine nitrogen is well established for ligands such as 6,6'-dimethyl-2,2'-bipyridine or 2,9-dimethyl-1,10-phenanthroline with copper,⁴⁹ such effects are much less well known for octahedral complexes.⁵⁰ The present results show the possibility of using this effect in the design of new ligands, either to introduce selectivity for larger or smaller metal ions or to tune metal redox potentials.

Acknowledgment. We thank Dr. E. R. Henry (Laboratory of Chemical Physics, NIDDK, NIH, Bethesda, MD) for providing the computer program SHELL. This work is supported through grants from the Swiss National Science Foundation.

Supplementary Material Available: Tables giving crystal data and details of the structure determination, hydrogen coordinates and thermal parameters, bond lengths, bond angles, least squares plane data, anisotropic displacement parameters, and interplane angles (24 pages). The numbering scheme used for [Co₂(6-bisbmbp)₃](ClO₄)₄(CH₃CN)_{2.5} (**6**) has been changed from that used in the preliminary communication²⁰ to be identical for that used for **7**. Ordering information is given on any current masthead page.

- (46) Wilkins, R. G. *Kinetics and Mechanisms of Reaction of Transition Metal Complexes*, 2nd ed.; VCH, Weinheim, New York, Basel, Cambridge, 1991; p 265.
 (47) Brunschwig, B. S.; Creutz, C.; Macartney, D. H.; Sham, T. K.; Sutin, N. *Faraday Discuss. Chem. Soc.* **1992**, *74*, 113-127.
 (48) Ferguson, J.; Hawkins, C. J.; Kane-Maguire, N. A. P.; Lip, H. *Inorg. Chem.* **1969**, *8*, 771-779. Yanagi, K.; Ohashi, Y.; Sasada, Y.; Kaizin, Y.; Kobayashi, H. *Bull. Chem. Soc. Jpn.* **1981**, *54*, 118-126. Yoshikawa, Y.; Yamasaki, K. *Coord. Chem. Rev.* **1979**, *28*, 205-229.
 (49) Federlin, P.; Kern, J.-M.; Rastegar, A.; Dietrich-Büchcker, C.; Marnot, P. A.; Sauvage, J.-P. *New J. Chem.* **1990**, *14*, 9-12.
 (50) Onggo, D.; Goodwin, H. A. *Aust. J. Chem.* **1991**, *44*, 1539-1551.